Available online at www.sciencedirect.com

SciVerse ScienceDirect

Ceramics International 39 (2013) 5145–5149

CERAMICS INTERNATIONAL

www.elsevier.com/locate/ceramint

Synthesis and electrochemical properties of La-doped $Li_4Ti_5O_{12}$ as anode material for Li-ion battery

Dan Wang[a,*], Chunming Zhang[a], Yaoyao Zhang[b], Jin Wang[a], Dannong He[a,b,*]

[a]National Engineering Research Center for Nanotechnology, Shanghai 200241, China
[b]School of Material Science and Engineering, Shanghai Jiaotong University, Shanghai 200240, China

Received 12 November 2012; received in revised form 4 December 2012; accepted 5 December 2012
Available online 12 December 2012

Abstract

La-doped $Li_4Ti_5O_{12}$ was successfully synthesized from Li_2CO_3, La_2O_3 and tetrabutyl titanate by a simple ball milling assisted modified solid-state method. The impact of La-doping on crystalline structure, particle size, morphology and electrochemical performance of $Li_4Ti_5O_{12}$ was investigated. The samples were characterized by XRD, SEM, galvanostatically charge–discharge and electrochemical impedance spectroscopy. The results demonstrated that the in-situ coated and ball-milling method could decrease the particle size and prevent the aggregation of $Li_4Ti_5O_{12}$. La-doping obviously improved the rate capability of $Li_4Ti_5O_{12}$ via the generation of less electrode polarization and higher electronic conductivity. $Li_{3.95}La_{0.05}Ti_5O_{12}$ exhibited a relatively excellent rate capability and cycling stability. At the charge–discharge rate of 0.5 C and 40 C, its discharge capacities were 176.8 mAh/g and 54.7 mAh/g. After 10 cycles, fairly stable cycling performance was achieved without obvious capacity fade at 0.5 C, 1 C, 2 C, 5 C, 10 C, 20 C and 40 C. In addition, compared to $Li_4Ti_5O_{12}$, $Li_{3.95}La_{0.05}Ti_5O_{12}$ almost did not have the initial capacity loss. It indicated that $Li_{3.95}La_{0.05}Ti_5O_{12}$ was a promising candidate material for anodes in Li-ion battery application.

Keywords: Li-ion battery; Anode materials; $Li_4Ti_5O_{12}$; Doping

1. Introduction

Nowadays, an ever-increasing research effort has been paying for rechargeable batteries for applications in electric vehicles and energy storage systems. These applications demand high power, high energy densities, high safety and long cycle-life. State-of-the-art lithium-ion batteries have been considered as an attractive power source for a wide variety of applications, due to their high power and energy densities. As a promising anode material for lithium-ion batteries, spinel $Li_4Ti_5O_{12}$ has attracted special attention due to its extremely small structural change during Li insertion/extraction, its high reversible capacity (175 mAh/g) and its flat discharge platform at about 1.55 V versus Li^+/Li [1–4]. This high voltage above the reduction potential of most organic electrolytes can restrain the passive films from the reduction of electrolytes and sufficiently avoid the formation of metallic lithium [5]. Therefore, $Li_4Ti_5O_{12}$ is much safer and more stable than carbon-based materials.

Despite the advantages mentioned above, however, there are some obstacles for the development and commercialization of $Li_4Ti_5O_{12}$. One of the main obstacles is its low electronic conductivity, which leads to its low rate capacity [6]. Three typical approaches have been developed over the past few years to resolve this problem. One is to improve the synthesis route to get nanoparticles, which can shorten the Li-ion diffusion path and broaden the electrode/electrolyte contact surface obviously [7–12]; another is to improve the electrical conductivity by surface modification with metals or their oxides [13,14], and carbon coating [15–18]; the other is to substitute Li or Ti by other metal cations [19–21].

The introduction of heteroatoms is a widely adopted promising method. The effects of the introduced heteroatoms on electrochemical performance are complicated depending on species and forms of heteroatoms, and

*Corresponding authors. Tel.: +86 21 34291286.
E-mail addresses: julian-wang@163.com (D. Wang), hdnbill@sh163.net (D. He).

0272-8842/$ - see front matter © 2012 Elsevier Ltd and Techna Group S.r.l. All rights reserved.
http://dx.doi.org/10.1016/j.ceramint.2012.12.010

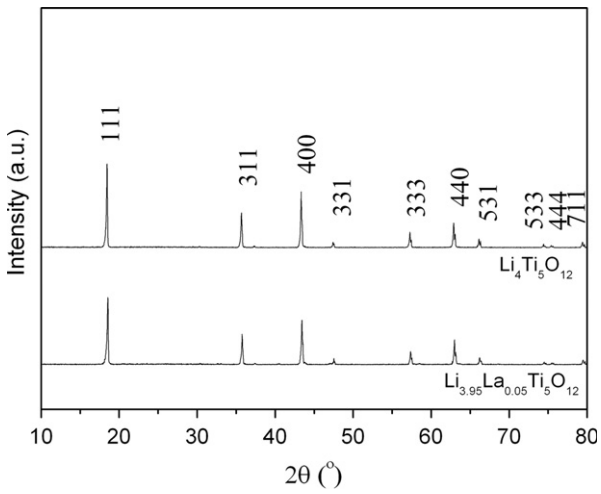

Fig. 1. XRD patterns of the $Li_4Ti_5O_{12}$ and the $Li_{3.95}La_{0.05}Ti_5O_{12}$.

parent structures [22,23]. Recently, Luo et al. [24] reported enhancing the electrochemical performance of $LiFePO_4$ electrodes by La ion doping. The method applied for $LiFePO_4$ offers a simple approach to synthesize $Li_4Ti_5O_{12}$ with high rate capacity. In this study, La doped $Li_4Ti_5O_{12}$ powders were prepared by a simple ball milling assisted modified solid-state method and the influence of La doped on the morphology and electrochemical performance of $Li_4Ti_5O_{12}$ were systematically investigated.

2. Experimental

$Li_{3.95}La_{0.05}Ti_5O_{12}$ was synthesized by a ball milling assisted solid-state reaction. Solution A was obtained by dissolving stoichiometric amount of Li_2CO_3 (AR) and La_2O_3 (AR) in a volume alcohol/deionized water ratio of 4:1. Solution B was obtained by dissolving stoichiometric amount of tetrabutyl titanate in alcohol. Solution B was added slowly into solution A. The dried precursor was obtained by filtering, washing, and drying the slurry mixture. The precursor was further calcined at the 800 °C for 7 h. The obtained powders were dispersed in the mixture solution of alcohol and deionized water and then well mixed by ball milling using agate balls and bowl at a ball-to-powders weight ratio of 3:1. The milling was performed in air at 400 rpm rotational speed for 10 h. The white slurry was dried to obtain the final powders. For comparison, the pure $Li_4Ti_5O_{12}$ powders were also prepared using similar method.

The crystal structure of the synthesized powders was examined by X-ray diffraction analysis (XRD, Model X'TRAX) using nickel filtered Cu-Ka radiation (λ=0.15406 nm) over the 2θ range from 10° to 80°. The particle morphology of the powders was observed using an S-4800 field emission scanning electron microscopy (SEM). Electrochemical properties of the samples were measured with the assembled swagelok cells, for which Li metal was used as a counter and reference electrode, the electrolyte was 1 M $LiPF_6$ in ethylene carbonate and diethyl carbonate (EC–DEC 1:1, v/v) and a Celgard2325 polypropylene micro-porous film was used as the separator. The electrode was prepared by mixing 85 wt% $Li_{3.95}La_{0.05}Ti_5O_{12}$ active material, 10 wt% carbon black (Super P) and 5 wt% polyvynilidene fluoride (PVDF) binder dispersed in enough N-methyl-2-pyrrolidine (NMP). Then, the viscous slurry was cast on the current collector of a copper foil by a blade. After drying overnight under vacuum at 100 °C to remove the solvent, the electrode was punched to a disk shape with a diameter of 12 mm for the half-cell test. The cell was assembled in a dry glove box filled with high purity argon gas. The galvanostatic discharge–charge tests were carried out using a Xinwei Instrument in the voltage range of 1.0 to 3.0 V versus Li^+/Li. Electrochemical impedance spectroscopy was performed by an electrochemical workstation (Shanghai Chenhua Instrument Co. Ltd., China) in the frequency range from 0.1 Hz to 1 MHz.

3. Results and discussion

The color of the synthesized powder is white. The XRD patterns of the $Li_4Ti_5O_{12}$ and $Li_{3.95}La_{0.05}Ti_5O_{12}$ are shown in Fig. 1.

The diffraction peaks conform to spinel $Li_4Ti_5O_{12}$ structure (JCPDS file no. 26-1198) without obvious impurity phase, which indicates that La^{3+} has successfully entered the lattice of the spinel and do not change its structure. The crystallite sizes of $Li_4Ti_5O_{12}$ and $Li_{3.95}La_{0.05}Ti_5O_{12}$ are calculated from the Scherrer formula $D=\beta\ \lambda/B\ \cos(\theta)$, where B is the full-width-at-half-maximum of the diffraction peaks, λ is the X-ray wavelength (0.15418 nm), β is a constant (0.89) and θ is the reflection angle of the peaks. Peaks at (111), (311) and (400) reflection are taken to evaluate the crystallite sizes of $Li_4Ti_5O_{12}$ and $Li_{3.95}La_{0.05}Ti_5O_{12}$ crystallites. The mean crystallite sizes of $Li_4Ti_5O_{12}$ and $Li_{3.95}La_{0.05}Ti_5O_{12}$ particles are 97.7 and 103.4 nm, respectively.

Fig. 2 shows SEM images of the undoped $Li_4Ti_5O_{12}$ powders and the La-doped powders. It is obvious that both powders exhibit a uniform particle size distribution. Generally, the crystallite size is about 400 nm in both samples, which is smaller than the $Li_4Ti_5O_{12}$ synthesized by the traditional solid-state method. These fine powders can be attributed to the modified solid-state method in which the starting materials are well-dispersed and $TiO_2 \cdot H_2O$ in-situ uniformly covers the Li_2CO_3 and La_2O_3 surfaces. As is seen in Fig. 2(a), the $Li_4Ti_5O_{12}$ sample appears as heavily aggregated micron-sized particles of about 1 μm in diameters, but the $Li_{3.95}La_{0.05}Ti_5O_{12}$ sample has no obvious aggregation. It is well known that the agglomerated particles can make the Li^+ insertion/extraction in individual $Li_4Ti_5O_{12}$ grains inhomogeneous. The $Li_4Ti_5O_{12}$ grains inside the densely packed particles might be inactive especially when being cycled at high current densities due to the increased Li^+ diffusion

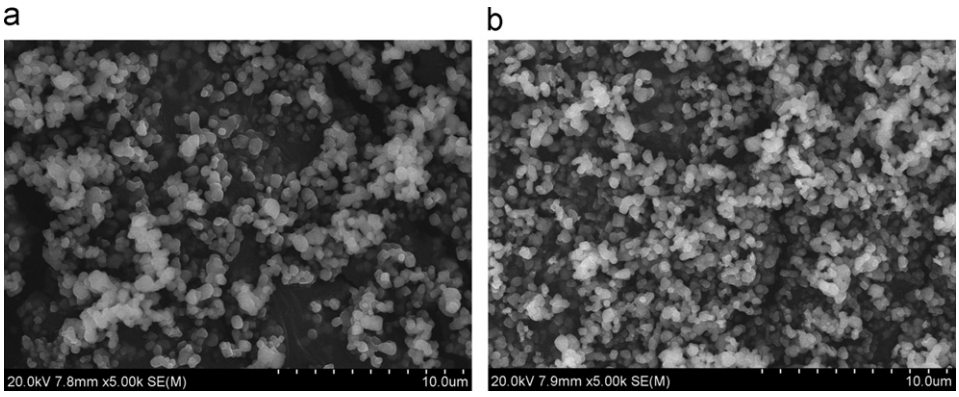

Fig. 2. SEM patterns of (a) the $Li_4Ti_5O_{12}$ and (b) the $Li_{3.95}La_{0.05}Ti_5O_{12}$.

distance. These results manifest that the La^{3+}-doping can help to hinder the agglomerate of $Li_4Ti_5O_{12}$ particles.

The electrochemical properties of the powders are determined by charge–discharge test at constant current density. Fig. 3 shows the initial discharge curves of the undoped and La-doped $Li_4Ti_5O_{12}$ powders at different rates from 0.5 to 40 C in potential window between 3.0 and 1.0 V. We can clearly see that the discharge voltage plateau drops with the current rate increasing for both the electrodes. The discharge plateau potentials at 0.5 C and 1 C are very close to the reversible redox potential of spinel $Li_4Ti_5O_{12}$ (1.55 V), as reported by Scharner et al. [25]. However, after the current rate increased, the discharge plateau becomes inconspicuous slow and even no obvious discharge plateaus can be found at 20 C and 40 C. The main reason is perhaps due to the high resistance of the electrode, which causes the high polarization of the electrode. Compared with the $Li_4Ti_5O_{12}$, the $Li_{3.95}La_{0.05}Ti_5O_{12}$ electrode exhibits an excellent rate capability, especially at high rates. The $Li_{3.95}La_{0.05}Ti_5O_{12}$ presents a discharge capacity of 176.8 mAh/g at 0.5 C. In contrast, the discharge capacity of the $Li_4Ti_5O_{12}$ is only 164.5 mAh/g. The discharge capacity of the $Li_{3.95}La_{0.05}Ti_5O_{12}$ is slightly higher than the theoretical capacity of the spinel $Li_4Ti_5O_{12}$ (175 mAh/g), which may be related to the carbon black as the electronic conductor during the electrode preparation. However, with increasing the discharge–charge current rate, the difference between the discharge capacities of these two samples becomes evident. At 40 C, the capacity of the $Li_4Ti_5O_{12}$ is only 30.2 mAh/g; however, the discharge capacity of the $Li_{3.95}La_{0.05}Ti_5O_{12}$ still remains 54.7 mAh/g. This improvement in the high rate capacity of the $Li_{3.95}La_{0.05}Ti_5O_{12}$ could be attributed to the improved electronic conductivity caused by a certain amount of Ti ions transferred from Ti^{4+} to Ti^{3+}, while La^{3+} doped [21].

The delithiation capacities of $Li_{3.95}La_{0.05}Ti_5O_{12}$ after 10 charge–discharge cycles are 174.7, 169.7, 160.6, 138.3, 110.9, 81.2 and 54.7 mAh/g at 0.5 C, 1 C, 2 C, 5 C, 10 C, 20 C and 40 C, respectively. The corresponding capacity fading rates at these C-rates are calculated to be 0.12%, 0.04%, 0.02%, 0.03%, 0.13%, 0.11% and 0.001% per cycle, which shows very high capacity retention. But the capacity-cycle profile of $Li_4Ti_5O_{12}$ shows a large fluctuation in capacity, which is not as smooth as that of the $Li_{3.95}La_{0.05}Ti_5O_{12}$, as shown in Fig. 4. We believe that a large portion of $Li_4Ti_5O_{12}$ grains in the aggregated particles cannot be fully utilized and become inactive due to a longer diffusion distance for the lithium ion and insufficient lithium ion diffusion at high rates, which inevitably decreases the discharge capacity. The lithium ion insertion/extraction mainly takes place on the outside of the large particles and individual lithium ion insertion/extraction in the aggregated particles at different cycles leads to the capacity fluctuation in the capacity-cycle

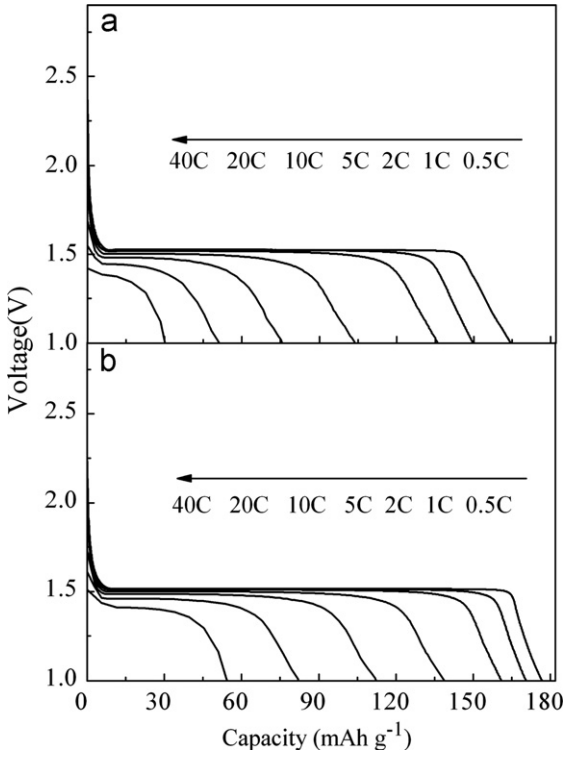

Fig. 3. The discharge curves of (a) $Li_4Ti_5O_{12}$ and (b) $Li_{3.95}La_{0.05}Ti_5O_{12}$ at different rates.

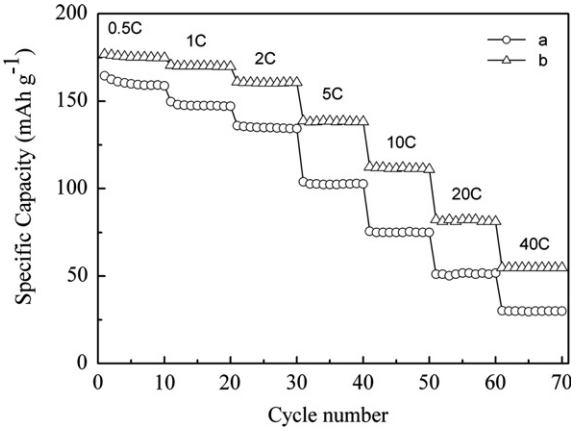

Fig. 4. The cyclic performance of (a) $Li_4Ti_5O_{12}$ and (b) $Li_{3.95}La_{0.05}Ti_5O_{12}$ at different rates.

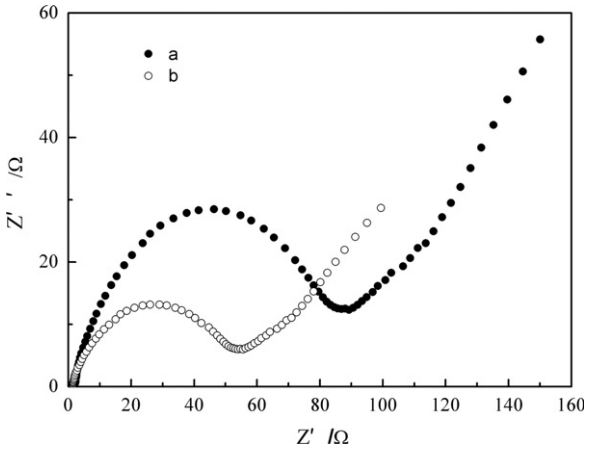

Fig.5. EIS results of (a) $Li_4Ti_5O_{12}$ and (b) $Li_{3.95}La_{0.05}Ti_5O_{12}$.

profile. The introduced heteroatoms can enhance reversible capacity and improve cycling behavior [22]. The good cycling stability of $Li_{3.95}La_{0.05}Ti_5O_{12}$ can be attributed to the La^{3+}-doping, which hinder the agglomerate and improve the electrical conductivity. In addition, it also could be clearly seen that $Li_{3.95}La_{0.05}Ti_5O_{12}$ almost has not the initial capacity loss. The specific cause will be investigated subsequently.

Electrochemical impedance spectroscopy (EIS) may be considered one of the most sensitive tools for studying the changes in the electrode behavior. To further demonstrate the effect of La^{3+}-doping on the electrode performance, the EIS of $Li_4Ti_5O_{12}$ and $Li_{3.95}La_{0.05}Ti_5O_{12}$ were measured. Fig. 5 shows the typical impedance spectra of both electrodes at room temperature. The impedance plots are composed of a depressed semicircle in the high frequency range and a spike in the low frequency range. It is well known that the cross-section value of impedance spectra on the real Z' axis at the high frequency is the internal resistance (R_i), R_i, corresponding the resistance of electrolyte mainly, while the semicircle is corresponding to the electrochemical reaction resistance and the double layer capacity of the electrode. The inclined line in the lower frequency range is attributed to the Warburg impedance, which is associated with lithium-ion diffusion through the $Li_4Ti_5O_{12}$ electrode [15]. As shown in Fig. 5, the $Li_{3.95}La_{0.05}Ti_5O_{12}$ electrode exhibits lower electrochemical reaction resistance, which is consistent with the result of better reversible capacities. It demonstrates that La^{3+}-doping can significantly improve the electrochemical kinetics of $Li_4Ti_5O_{12}$ samples and decrease their resistance. Such improvement may be associated with the improvement of the charge transfer process over the electrode surface, which can increase the electronic conductivity of $Li_4Ti_5O_{12}$ arising from La^{3+}-doping.

4. Conclusions

$Li_{3.95}La_{0.05}Ti_5O_{12}$ powders have been successfully synthesized by a simple ball milling assisted modified solid-state method. XRD patterns show that the $Li_{3.95}La_{0.05}Ti_5O_{12}$ has good crystallinity and high phase purity. The $Li_{3.95}La_{0.05}Ti_5O_{12}$ electrode presents a higher specific capacity and better cycling performance than the $Li_4Ti_5O_{12}$ electrode prepared by the similar process. $Li_{3.95}La_{0.05}Ti_5O_{12}$ exhibits a specific capacity of 174.7 mAh/g at 0.5 C and 110.9 mAh/g at 10 C after 10 cycles. Furthermore, $Li_{3.95}La_{0.05}Ti_5O_{12}$ has been proved to be a high rate anode material with higher electronic conductivity and lithium-ion diffusivity than the $Li_4Ti_5O_{12}$, implying that La-doping is beneficial to the reversible intercalation and extraction of Li^+. All the evidences demonstrate that the $Li_{3.95}La_{0.05}Ti_5O_{12}$ electrode is a promising anode material for Li-ion batteries.

Acknowledgments

This work was supported by the National Science Foundation of China (No. 21171116) and International Science & Technology Cooperation Program of China (No. 2012DFG11660).

References

[1] K.M. Colbow, J.R. Dahn, R.R. Haering, Structure and electrochemistry of the spinel oxides $LiTi_2O_4$ and $LiTiO_4$, Journal of Power Sources 26 (1989) 397–402.
[2] T. Yuan, R. Cai, R. Ran, Y.K. Zhou, Z.P. Shao, A mechanism study of synthesis of $Li_4Ti_5O_{12}$ from TiO_2 anatase, Journal of Alloys and Compounds 505 (2010) 367–373.
[3] G.F. Yan, H.S. Fang, H.J. Zhao, G.S Li, Y. Yang, L.P. Li, Ball milling-assisted sol–gel route to $Li_4Ti_5O_{12}$ and its electrochemical properties, Journal of Alloys and Compounds 470 (2009) 544–547.
[4] L.X. Yang, L.J. Gao, $Li_4Ti_5O_{12}$/C composite electrode material synthesized involving conductive carbon precursor for Li-ion battery, Journal of Alloys and Compounds 485 (2009) 93–97.
[5] X.B. Hu, Z.J. Lin, K.R. Yang, Z.H. Deng, J.S. Suo, Influence factors on electrochemical properties of $Li_4Ti_5O_{12}$/C anode material pyrolyzed from lithium polyacrylate, Journal of Alloys and Compounds 506 (2010) 160–166.
[6] C.H. Chen, J.T. Vaughey, A.N. Jansen, D.W. Dees, A.J. Kahaian, T. Goacher, M.M. Thackeray, Studies of Mg-substituted $Li_{4-x}Mg_xTi_5O_{12}$

spinel electrodes ($0 < x < 1$) for lithium batteries, Journal of the Electrochemical Society 148 (2001) A102–A104.
[7] S.W. Han, J.W. Shin, D.H. Yoon, Synthesis of pure nano-sized $Li_4Ti_5O_{12}$ powder via solid-state reaction using very fine grinding media, Ceramics International 38 (2012) 6963–6968.
[8] A. Singhal, G. Skandan, G. Amatucci, F. Badway, N. Ye, A. Manthiram, H. Ye, J.J. Xu, Nanostructured electrodes for next generation rechargeable electrochemical devices, Journal of Power Sources 129 (2004) 38–44.
[9] Y.F. Tang, L. Yang, Z. Qiu, J.S. Huang, Preparation and electrochemical lithium storage of flower-like spinel $Li_4Ti_5O_{12}$ consisting of nanosheets, Electrochemistry Communications 10 (2008) 1513–1516.
[10] T. Yuan, R. Cai, K. Wan, R. Ran, S.M. Liu, Z.P. Shao, Combustion synthesis of high-performance $Li_4Ti_5O_{12}$ for secondary Li-ion battery, Ceramics International 35 (2009) 1757–1768.
[11] C.H. Hong, A. Noviyanto, J.H. Ryu, J. Kim, D.H. Yoon, Effects of the starting materials and mechanochemical activation on the properties of solid-state reacted $Li_4Ti_5O_{12}$ for lithium ion batteries, Ceramics International 38 (2012) 301–310.
[12] D. Wang, H.Y. Xu, M. Gu, C.H. Chen, $Li_2CuTi_3O_8$–$Li_4Ti_5O_{12}$ double spinel anode material with improved rate performance for Li-ion batteries, Electrochemistry Communications 11 (2009) 50–53.
[13] S.H. Huang, Z.Y. Wen, B. Lin, J.D. Han, X.G. Xu, The high-rate performance of the newly designed $Li_4Ti_5O_{12}$/Cu composite anode for lithium ion batteries, Journal of Alloys and Compounds 457 (2008) 400–403.
[14] S.H. Huang, Z.Y. Wen, J.C. Zhang, X.L. Yang, Improving the electrochemical performance of $Li_4Ti_5O_{12}$/Ag composite by an electroless deposition method, Electrochimica Acta 52 (2007) 3704–3708.
[15] J.J. Huang, Z.Y. Jiang, The preparation and characterization of $Li_4Ti_5O_{12}$/carbon nano-tubes for lithium ion battery, Electrochimica Acta 53 (2008) 7756–7759.
[16] G.J. Wang, J. Gao, L.J. Fu, N.H. Zhao, Y.P. Wu, T. Takamura, Preparation and characteristic of carbon-coated $Li_4Ti_5O_{12}$ anode material, Journal of Power Sources 174 (2007) 1109–1112.
[17] L. Cheng, X.L. Li, H.J. Liu, H.M. Xiong, P.W. Zhang, Y.Y. Xia, Carbon-coated $Li_4Ti_5O_{12}$ as a high rate electrode material for Li-ion intercalation, Journal of the Electrochemical Society 154 (2007) A692–A697.
[18] J. Gao, J.R. Ying, C.Y. Jiang, C.R. Wan, High-density spherical $Li_4Ti_5O_{12}$/C anode material with good rate capability for lithium ion batteries, Journal of Power Sources 166 (2007) 255–259.
[19] S.H. Huang, Z.Y. Wen, X.J. Zhu, Z.X. Lin, Effects of dopant on the electrochemical performance of $Li_4Ti_5O_{12}$ as electrode material for lithium ion batteries, Journal of Power Sources 165 (2007) 408–412.
[20] H.L. Zhao, Y. Li, Z.M. Zhu, J. Lin, Z.H. Tian, R.L. Wang, Structural and electrochemical characteristics of $Li_{4-x}Al_xTi_5O_{12}$ as anode material for lithium-ion batteries, Electrochimica Acta 53 (2008) 7079–7083.
[21] J. Wolfenstine, J.L. Allen, Electrical conductivity and charge compensation in Ta doped $Li_4Ti_5O_{12}$, Journal of Power Sources 180 (2008) 582–585.
[22] Y.P. Wu, Elke Rahm, Rudolf Holze, Effects of heteroatoms on electrochemical performance of electrode materials for lithium ion batteries, Electrochimica Acta 47 (2002) 3491–3507.
[23] T.F. Yi, L.J. Jiang, J. Shu, C.B. Yue, R.S. Zhu, H.B. Qiao, Recent development and application of $Li_4Ti_5O_{12}$ as anode material of lithium ion battery, Journal of Physics and Chemistry of Solids 71 (2001) 1236–1242.
[24] S.H. Luo, Z.L. Tang, J.B. Lu, Z.T. Zhang, Physical and electrochemical properties of La-doped lithium iron phosphate electrodes, Rare Metal Materials and Engineering 36 (2007) 1366–1368.
[25] S. Scharner, W. Weppner, P. Schmid-Beurmann, Evidence of two-phase formation upon lithium insertion into the $Li_{1.33}Ti_{1.67}O_4$ spinel, Journal of the Electrochemical Society 146 (1999) 857–861.